

## Supporting Information

### Oxygen Extrusion from Amide Ligands to Generate Terminal Ta=O Units Under Reducing Conditions. How to Successfully Use Amide Ligands in Dinitrogen Coordination Chemistry

Patricia Horrillo-Martinez, Brian O. Patrick, Laurel L. Schafer\* and Michael D. Fryzuk\*

University of British Columbia, Department of Chemistry, 2036 Main Mall,  
Vancouver, BC, V6T 1Z1

**General Considerations for X-ray Crystal Structure Determination.** X-ray data were collected on a Bruker X8 Apex II diffractometer with graphite-monochromated Mo K $\alpha$  radiation ( $\lambda = 0.71073 \text{ \AA}$ ) integrated using the Bruker SAINT software package.<sup>1</sup> The data were collected at a temperature of  $-170.0 \pm 0.1^\circ\text{C}$ . Absorption corrections for **3b,c**, **4**, **7b** and Cp\*TaMe<sub>4</sub> were performed using the multiscan technique (SADABS).<sup>2</sup> The structures were solved by direct methods<sup>3</sup> and refined using all reflections with the WinGX (version 1.80.05) software package.<sup>4</sup> All non-hydrogen atoms were refined anisotropically. All hydrogen atoms were included in calculated positions but not refined.

Crystals of **3a** were non-merohedrally twinned. Both twin domains are related by a 180° rotation about the (1 0 1) crystal axis. Data were integrated for both twin components, including both overlapped and non-overlapped reflections. In total 34875 reflections were integrated (15898 from component one only, 15745 from component two only, 3232 overlapped). The linear absorption coefficient,  $\mu$ , for Mo-K $\alpha$  radiation is 54.56 cm<sup>-1</sup>. Data were corrected for absorption effects using the multi-scan technique (TWINABS),<sup>5</sup> with minimum and maximum transmission coefficients of 0.419 and 0.549, respectively. The data were corrected for Lorentz and polarization effects. The structure was solved by direct methods<sup>3</sup> using non-overlapped data from the major twin component. Subsequent refinements were carried out using an HKLF 5 format data set containing complete data from both component 1 and component 2. The material crystallizes disordered about a pseudo-mirror plane passing through the Ta atom. The batch scale refinement showed a roughly 59:41 ratio between the major and minor twin components. The final cycle of full-matrix least-squares refinement on F<sup>2</sup> was based on 9240 reflections and 434

variable parameters and converged (largest parameter shift was 0.00 times its esd) with unweighted and weighted agreement factors of:

$$R1 = \sum |Fo| - |Fc| / \sum |Fo| = 0.044$$

$$wR2 = [ \sum (w(Fo^2 - Fc^2)^2) / \sum w(Fo^2)^2 ]^{1/2} = 0.068$$

The standard deviation of an observation of unit weight was 1.12. The weighting scheme was based on counting statistics. The maximum and minimum peaks on the final difference Fourier map corresponded to 1.42 and  $-1.71 \text{ e}^-/\text{\AA}^3$ , respectively. Neutral atom scattering factors were taken from Cromer and Waber.<sup>6</sup> Anomalous dispersion effects were included in  $F_{\text{calc}}$ ;<sup>7</sup> the values for  $\Delta f$  and  $\Delta f'$  were those of Creagh and McAuley.<sup>8</sup> The values for the mass attenuation coefficients are those of Creagh and Hubbell.<sup>9</sup> All refinements were performed using the SHELXTL<sup>10</sup> crystallographic software package of Bruker-AXS.

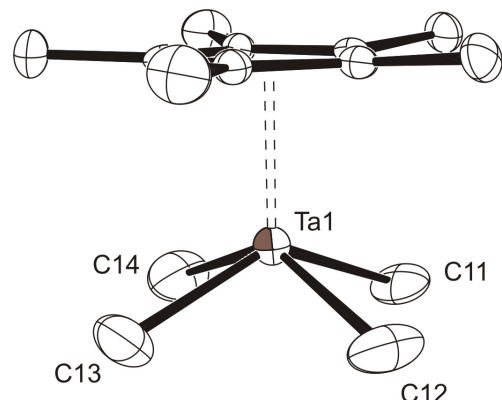


**Figure S1.** ORTEP representation of the solid-state molecular structure of  $\text{Cp}^*\text{TaMe}_4$  (ellipsoids at 50 % probability, hydrogens omitted for clarity) with selected bond lengths ( $\text{\AA}$ ): Ta1–C11, 2.156(7); Ta1–C12, 2.159(8); Ta1–C13, 2.141(7); Ta1–C14, 2.146(7).

## References

1. SAINT, Version 7.56, Bruker AXS Inc., Madison, Wisconsin, USA (2008).
2. SADABS, Bruker area detector scaling and absorption correction - Version 2008/1, Bruker AXS Inc., Madison, Wisconsin, USA (2008).
3. SIR97 - Altomare A., Burla M.C., Camalli M., Casciaro G.L., Giacovazzo C. , Guagliardi A., Moliterni A.G.G., Polidori G., Spagna R. (1999) *J. Appl. Cryst.* 32, 115-119.
4. L. J. Farrugia, *J. Appl. Cryst.* 1999, 32, 837-838.
5. Bruker Nonius scaling and absorption for twinned crystals – V2008/2, Bruker AXS Inc., Madison, Wisconsin, USA (2007).

6. Cromer, D. T. & Waber, J. T.; "International Tables for X-ray Crystallography", Vol. IV, The Kynoch Press, Birmingham, England, Table 2.2 A (1974).
7. Ibers, J. A. & Hamilton, W. C.; Acta Crystallogr., 17, 781 (1964).
8. Creagh, D. C. & McAuley, W.J.; "International Tables for Crystallography", Vol C, (A.J.C. Wilson, ed.), Kluwer Academic Publishers, Boston, Table 4.2.6.8, pages 219-222 (1992).
9. Creagh, D. C. & Hubbell, J.H.; "International Tables for Crystallography", Vol C, (A.J.C. Wilson, ed.), Kluwer Academic Publishers, Boston, Table 4.2.4.3, pages 200-206 (1992).
10. SHELXTL Version 5.1. Bruker AXS Inc., Madison, Wisconsin, USA. (1997).

**Table S1.** X-ray diffraction crystal data and structure refinement for  $\text{Cp}^*\text{Ta}(\text{amide})\text{Cl}_3$  **3a-c**.

	<b>3a</b>	<b>3b</b>	<b>3c</b>
formula	$\text{C}_{18}\text{H}_{31}\text{Cl}_3\text{NOTa}$	$\text{C}_{23}\text{H}_{33}\text{Cl}_3\text{NOTa}$	$\text{C}_{25}\text{H}_{29}\text{Cl}_3\text{NOTa}$
$F_w$	564.74	626.80	646.79
crystal size (mm)	0.11 x 0.17 x 0.23	0.30 x 0.30 x 0.50	0.10 x 0.20 x 0.50
colour, habit	yellow, prism	yellow-orange, prism	yellow, prism
cell setting	monoclinic	monoclinic	triclinic
space group	P21/n	P21/n	P-1
$a$ (Å)	10.0873(6)	11.665(2)	8.776(5)
$b$ (Å)	20.5258(11)	15.049(3)	12.131(5)
$c$ (Å)	10.5215(6)	28.516(5)	12.167(5)
$\alpha$ (°)	90	90	95.859(5)
$\beta$ (°)	96.685(3)	100.859(10)	90.822(5)
$\gamma$ (°)	90	90	109.198(5)
$V$ (Å <sup>3</sup> )	2163.7(2)	4916.2(15)	1215.3(10)
$Z$	4	8	2
$\rho_{\text{calcd}}$ (g cm <sup>-1</sup> )	1.734	1.694	1.767
$F(000)$	1112	2480	636
$\mu$ (MoK $\alpha$ ) (cm <sup>-1</sup> )	5.456	4.812	4.870
$2\theta_{\text{max}}$ (°)	55.12	60.08	55.12
total no. of reflns	9240	87918	19180
no. of unique reflns	9240 ( $R_{\text{int}} = 0.0000$ )	14191 ( $R_{\text{int}} = 0.0582$ )	5498 ( $R_{\text{int}} = 0.0286$ )
no. of reflns with $I > 2\sigma(I)$	7565	12220	5011
no. of variables	434	542	287
$R_1$ ( $F^2$ , all data)	0.0502	0.0755	0.0310
$wR_2$ ( $F^2$ , all data)	0.0630	0.1607	0.0671
$R_1$ ( $F$ , $I = 2\sigma(I)$ )	0.0336	0.0643	0.0253
$wR_2$ ( $F$ , $I = 2\sigma(I)$ )	0.0595	0.1563	0.0639
goodness of fit	1.195	1.267	1.075

**Table S2.** X-ray diffraction crystal data and structure refinement for **4a**, **7b** and  $\text{Cp}^*\text{TaMe}_4$ .

	<b>4a</b>	<b>4b</b>	<b>7b</b>	$\text{Cp}^*\text{TaMe}_4$
formula	$\text{C}_{18}\text{H}_{31}\text{Cl}_1\text{NOTa}$	$\text{C}_{23}\text{H}_{33}\text{ClNO}_2\text{Ta}$	$\text{C}_{46}\text{H}_{66}\text{Cl}_2\text{N}_4\text{O}_2\text{Ta}_2$	$\text{C}_{14}\text{H}_{27}\text{Ta}$
$F_w$	493.84	555.90	1139.84	376.31
crystal size (mm)	0.2 x 0.4 x 0.5	0.5 x 0.3 x 0.3	0.2 x 0.2 x 0.1	0.2 x 0.2 x 0.2
colour, habit	colorless, prism	colorless, cube	red, prism	yellow, prism
cell setting	monoclinic	monoclinic	triclinic	Orthorombic
space group	P21/n	P21/c	P-1	cmea
<i>a</i> (Å)	8.9863(4)	8.4087(8)	10.798(2)	13.8058(7)
<i>b</i> (Å)	19.3004(9)	19.2914(17)	18.392(4)	15.1978(7)
<i>c</i> (Å)	11.7122(5)	22.039(2)	28.086(6)	14.0101(6)
$\alpha$ (°)	90	90	93.870(10)	90
$\beta$ (°)	108.886(2)	94.868(3)	93.340(10)	90
$\gamma$ (°)	90	90	90.310(10)	90
<i>V</i> (Å <sup>3</sup> )	1921.99(15)	3562.2(6)	5555(2)	2939.6(2)
<i>Z</i>	4	4	2	8
$\rho_{\text{calcd}}$ (g cm <sup>-3</sup> )	1.707	1.419	1.528	1.701
<i>F</i> (000)	976	1552	2564	1472
$\mu$ (Mo $\kappa\alpha$ ) (cm <sup>-1</sup> )	5.860	3.192	4.075	7.451
$2\theta_{\text{max}}$ (°)	60.30	59.92	56.1	55.8
total no. of reflns	21963	39833	105750	8384
no. of unique reflns	5671 ( $R_{\text{int}} = 0.0279$ )	10316 ( $R_{\text{int}} = 0.0429$ )	26492 ( $R_{\text{int}} = 0.0732$ )	1828 ( $R_{\text{int}} = 0.0212$ )
no. of reflns with $I > 2\sigma(I)$	4970	8920	19547	1680
no. of variables	209	397	1241	169
$R_1(F^2, \text{all data})$	0.0258	0.0299	0.0608	0.0233
$wR_2(F^2, \text{all data})$	0.0483	0.0496	0.0764	0.0472
$R_1(F, I = 2\sigma(I))$	0.0199	0.0224	0.0356	0.0202

$wR_2 (F, I = 2\sigma(I))$	0.0464	0.0472	0.0681	0.0455
goodness of fit	1.038	1.029	0.995	1.035

Supplementary crystallographic data can be obtained free of charge from the Cambridge Crystallographic Data Centre via  
[www.ccdc.cam.ac.uk/data\\_request/cif](http://www.ccdc.cam.ac.uk/data_request/cif).

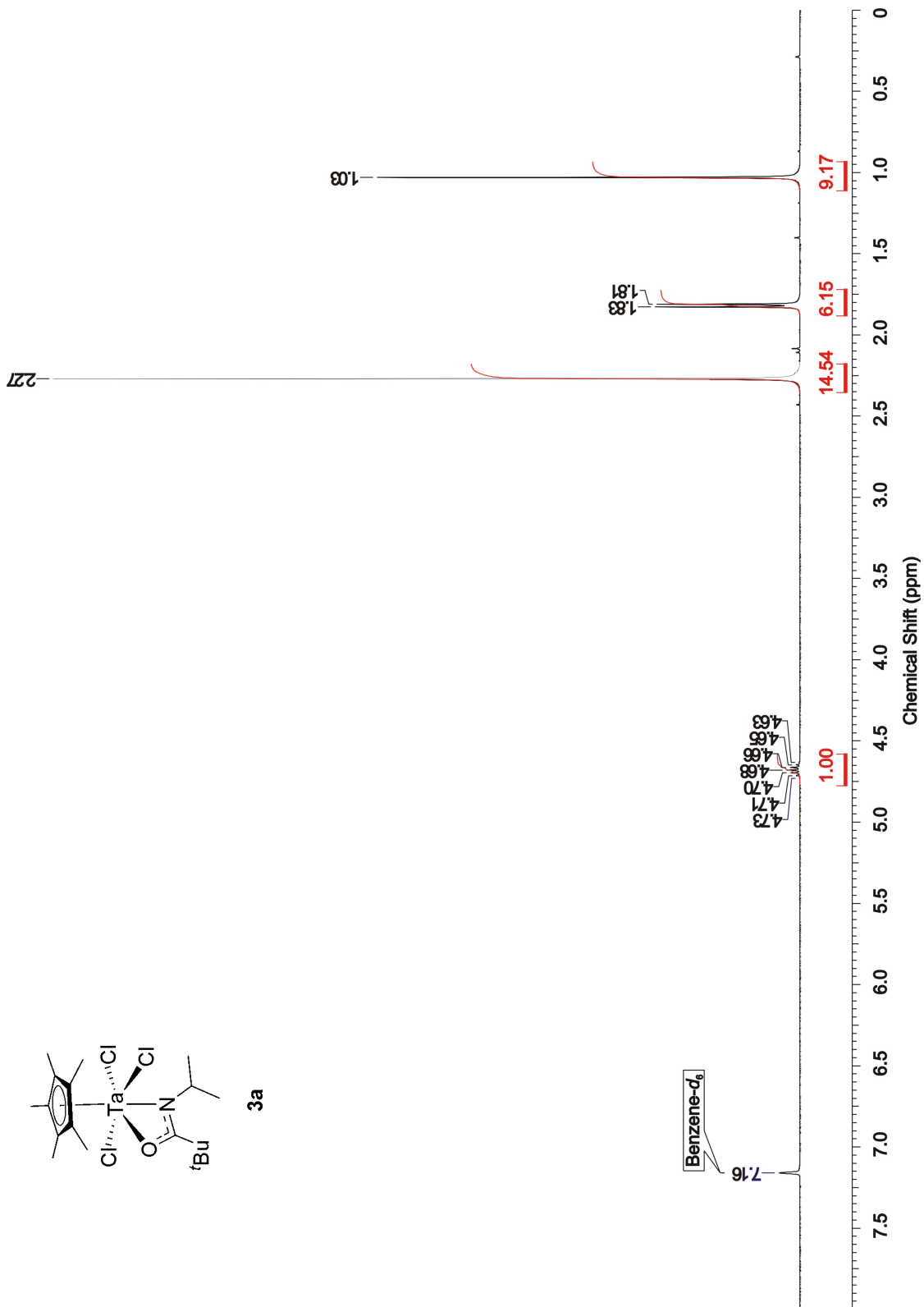
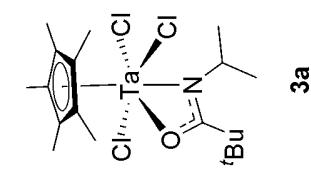


**Figure S2.**  $^1\text{H}$  NMR spectrum (400MHz, RT) of **3a** in benzene- $d_6$ .

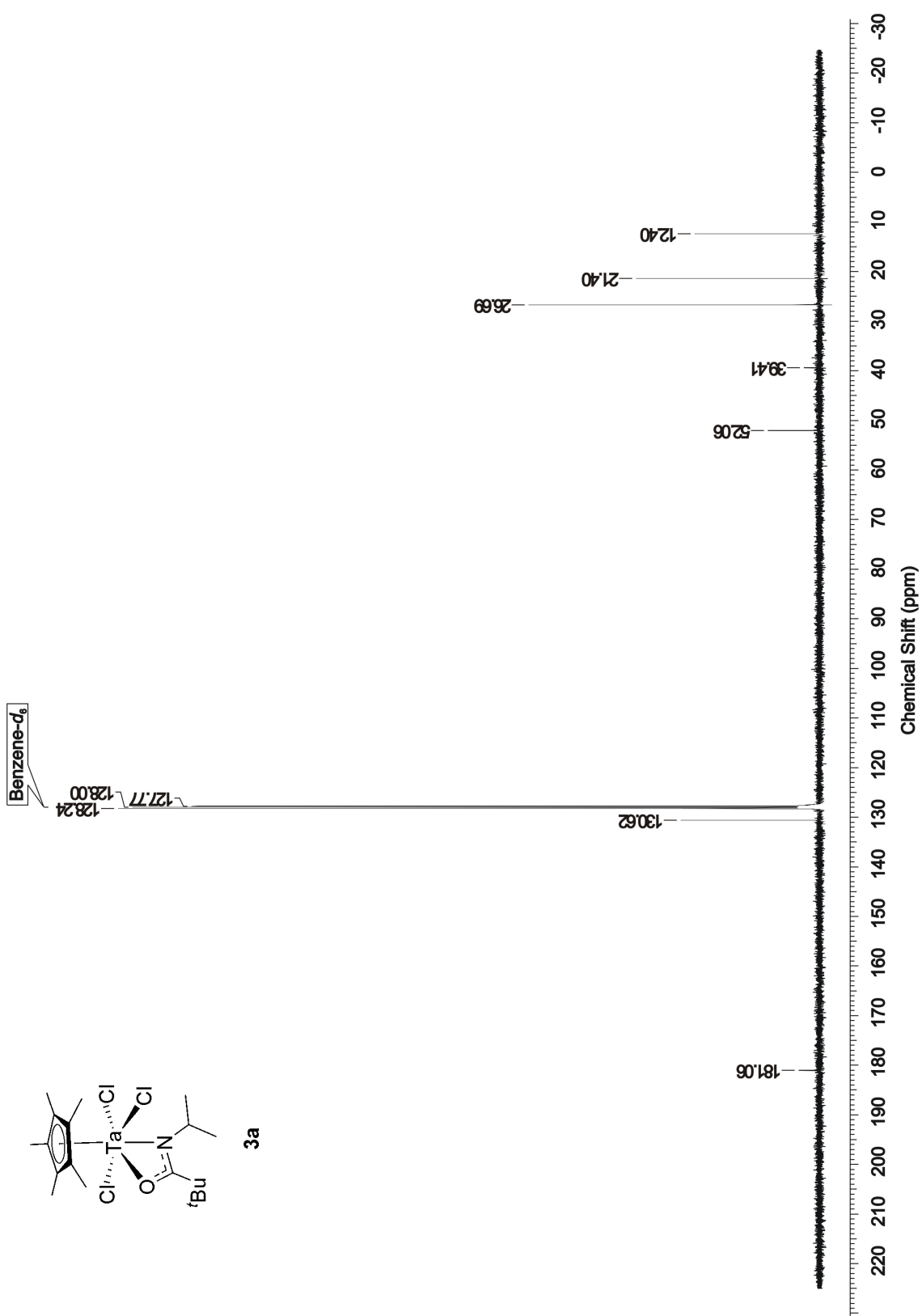
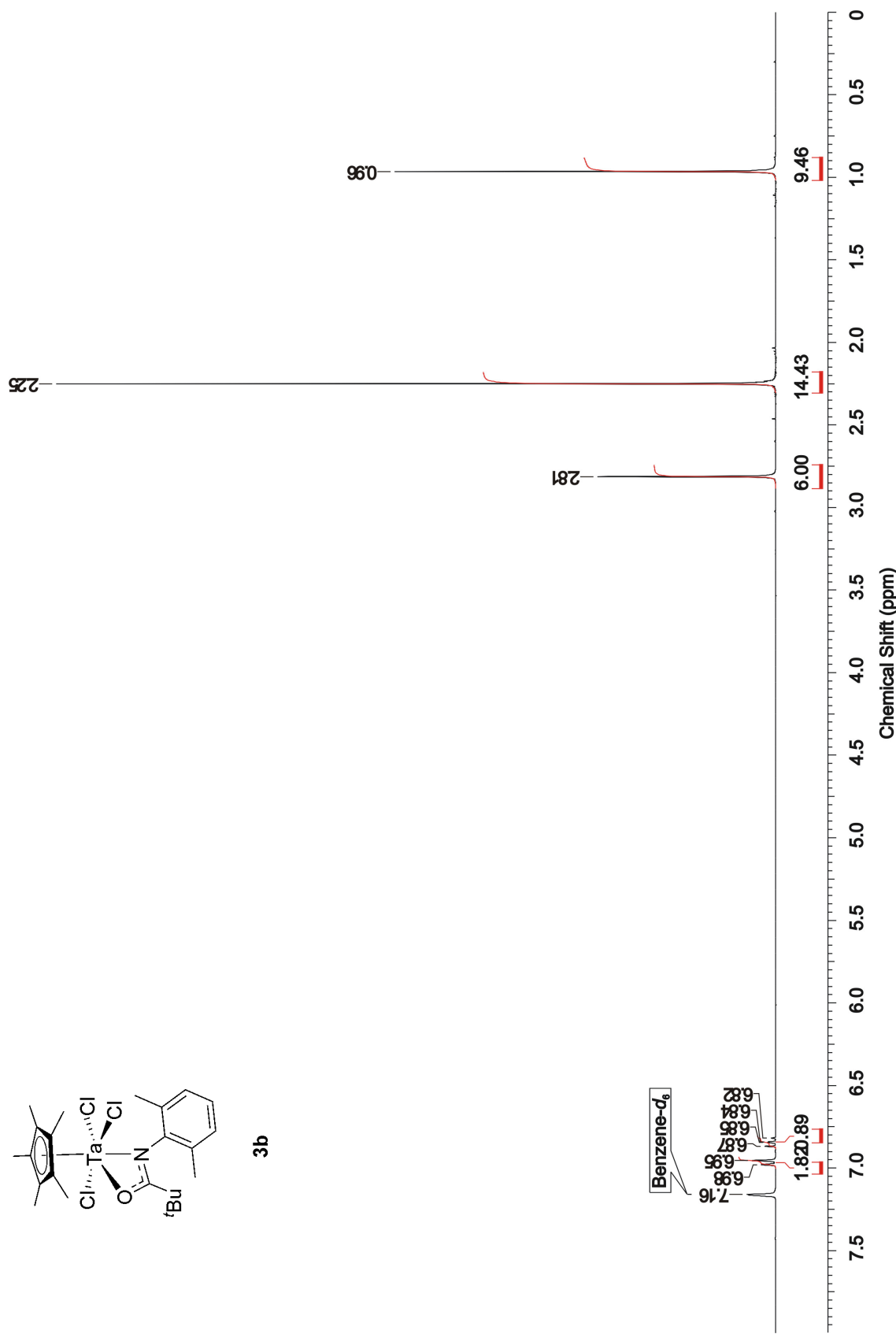
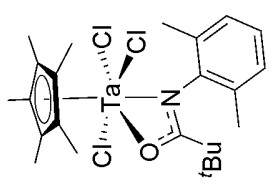


Figure S3.  $^{13}\text{C}$  NMR spectrum (100.6MHz, RT) of **3a** in benzene- $d_6$ .



**Figure S4.**  $^1\text{H}$  NMR spectrum (400MHz, RT) of **3b** in benzene-*d*<sub>6</sub>.

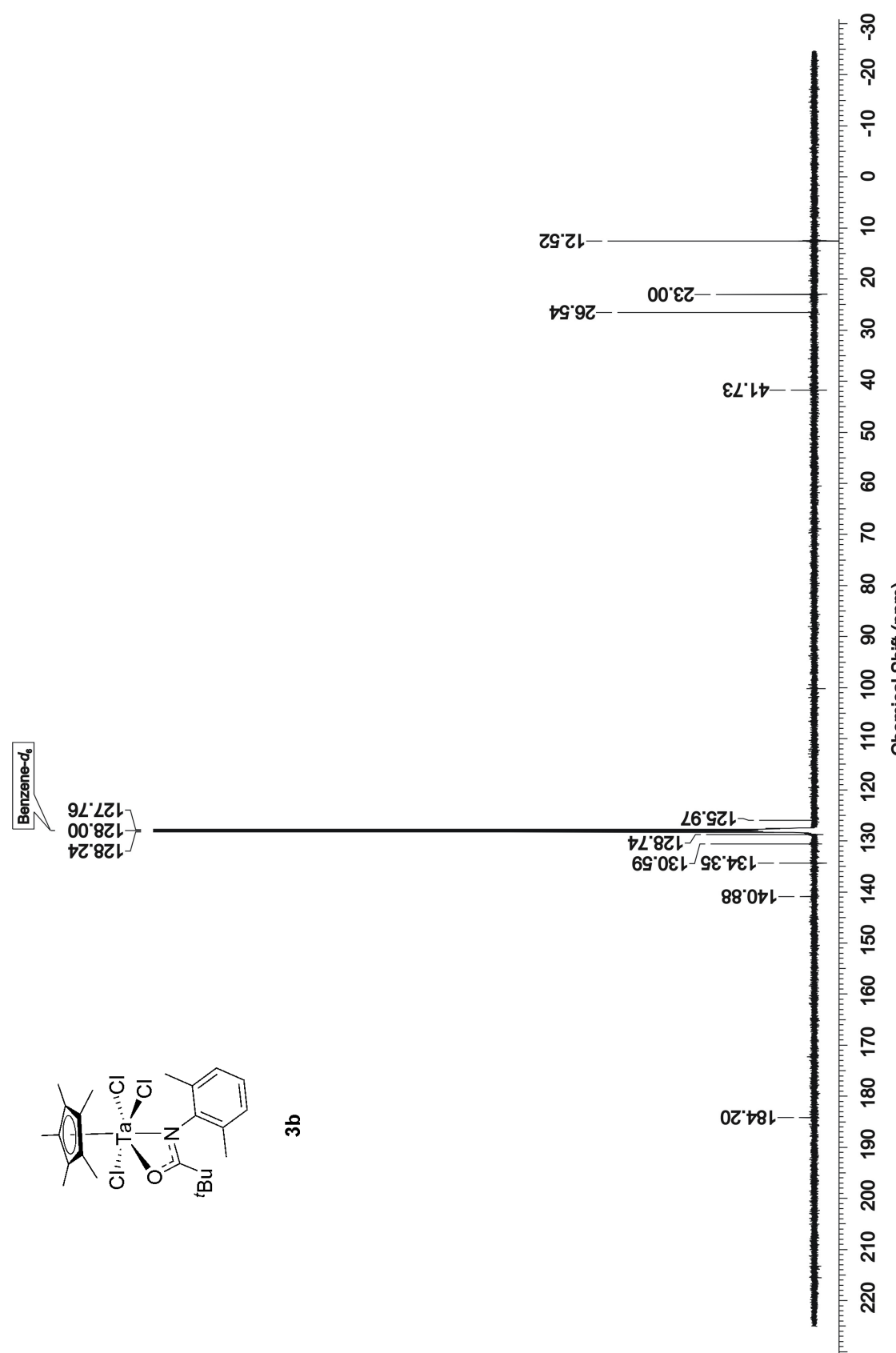
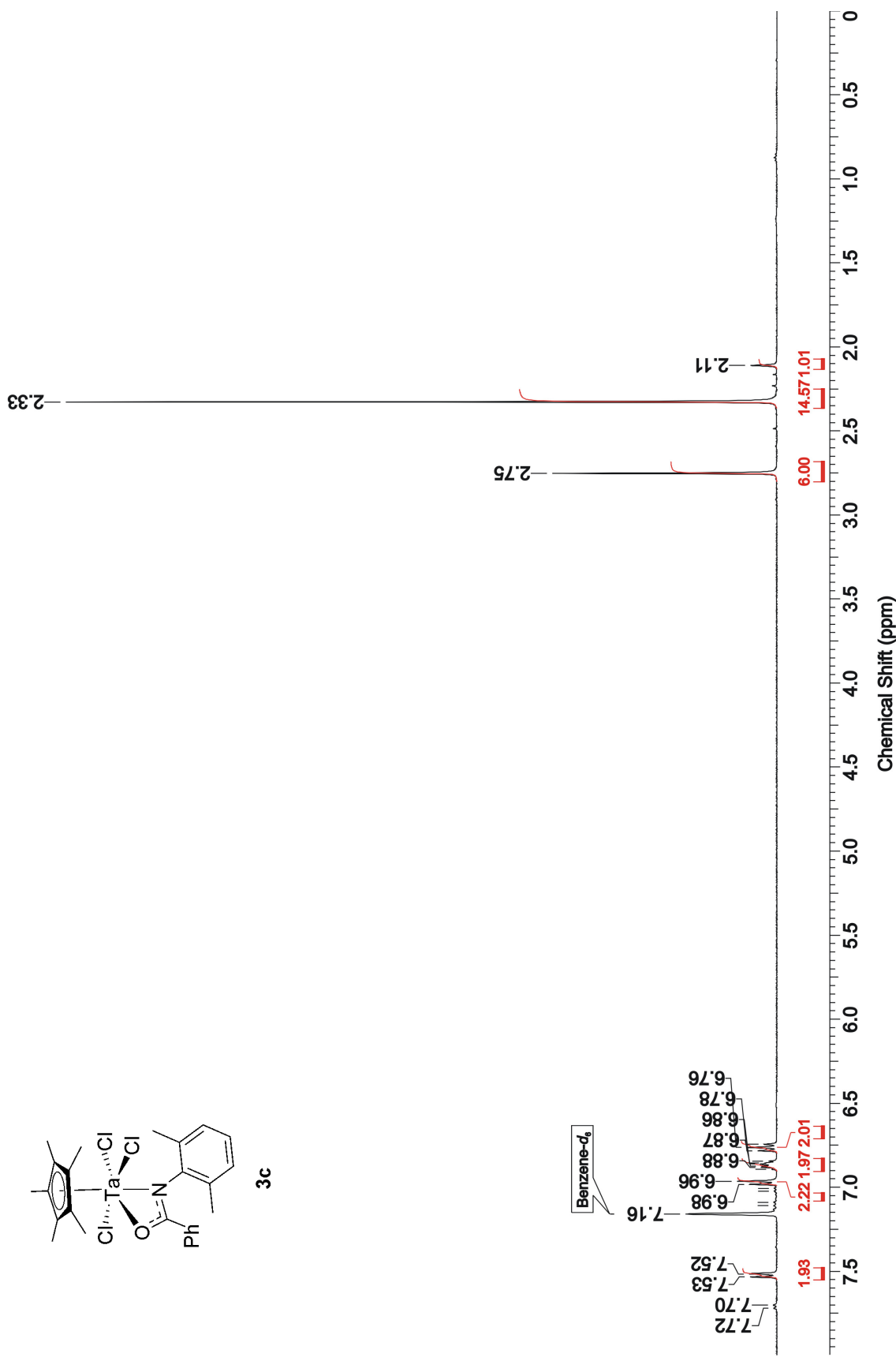
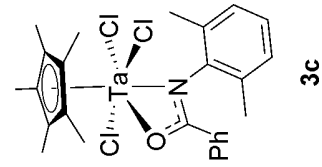


Figure S5.  $^{13}\text{C}$  NMR spectrum (100.6 MHz, RT) of **3b** in benzene- $d_6$ .



**Figure S6.**  $^1\text{H}$  NMR spectrum (400MHz, RT) of **3c** in benzene-*d*<sub>6</sub>.

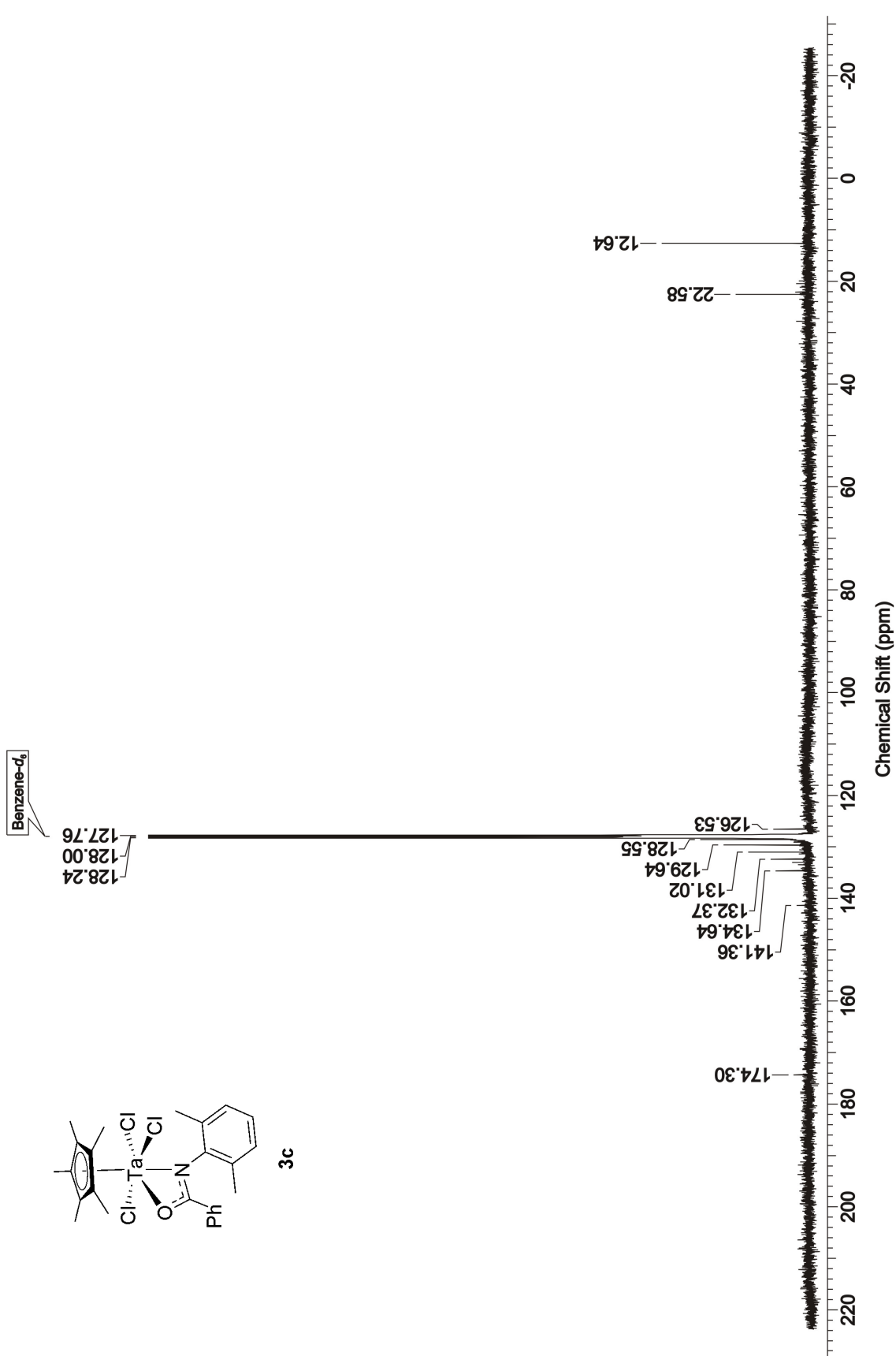


Figure S7.  $^{13}\text{C}$  NMR spectrum (100.6 MHz, RT) of **3c** in benzene- $d_6$ .

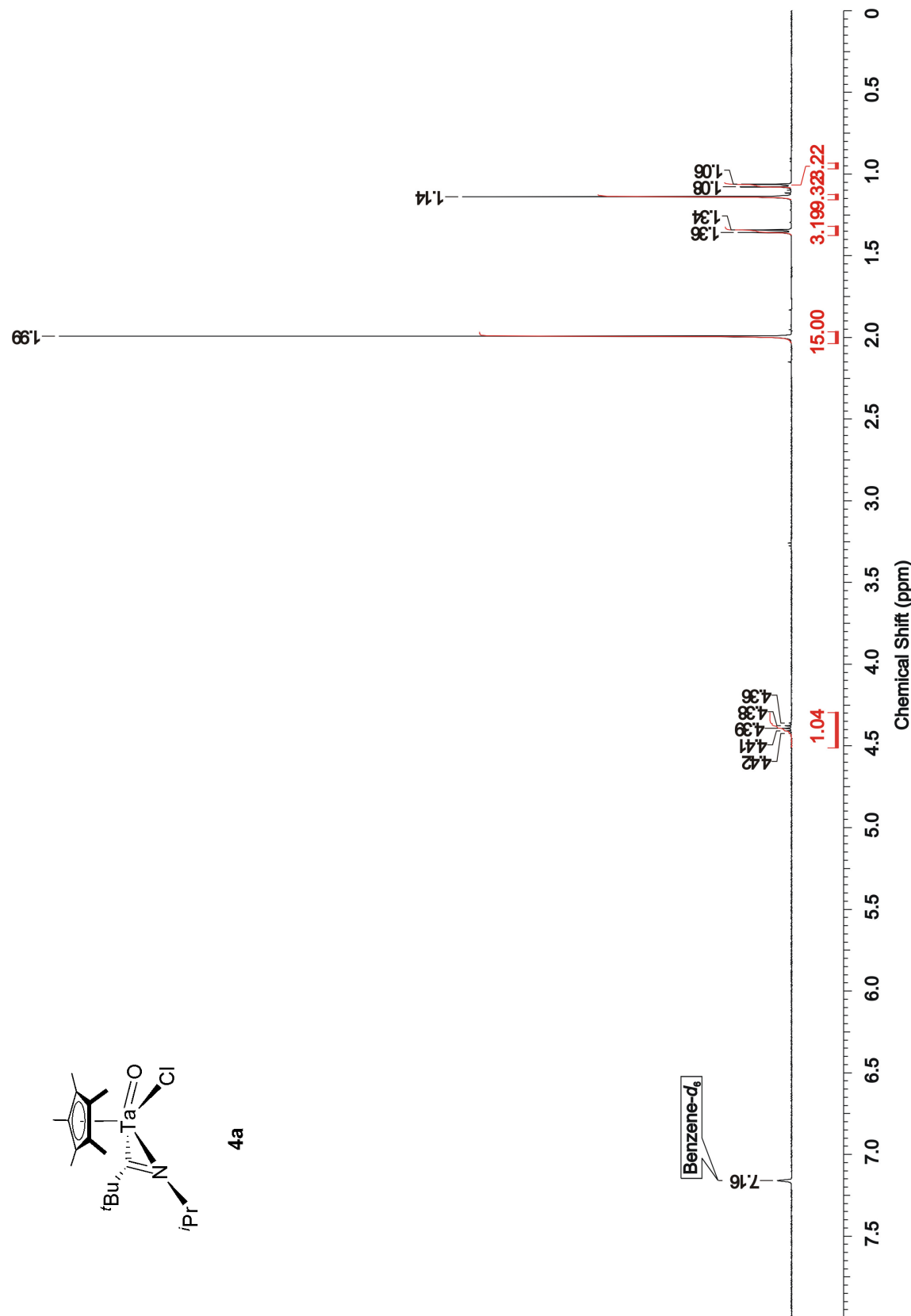


Figure S8.  $^1\text{H}$  NMR spectrum (400MHz, RT) of **4a** in benzene- $d_6$ .

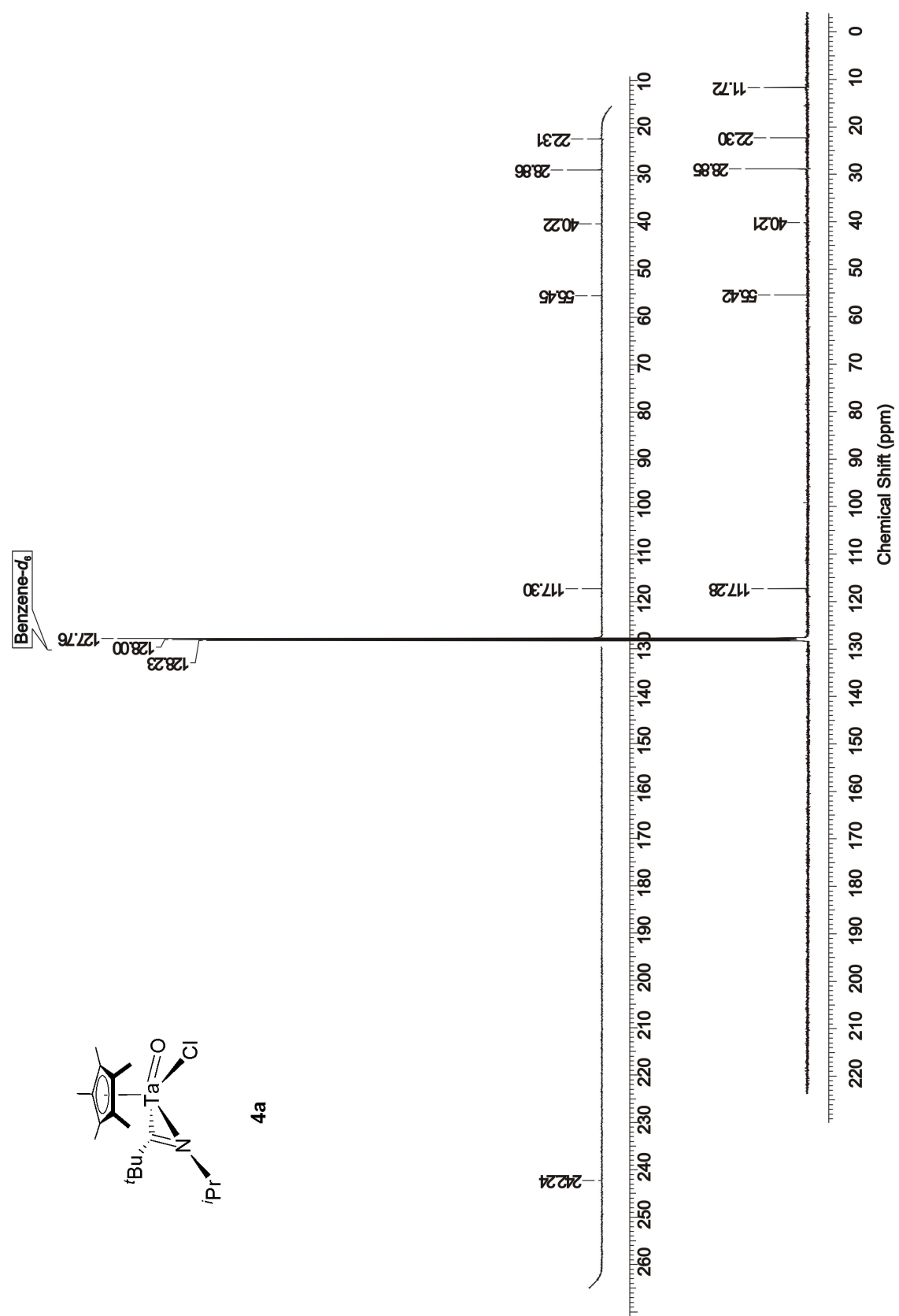


Figure S9.  $^{13}\text{C}$  NMR spectrum (100.6 MHz, RT) of **4a** in benzene- $d_6$ .

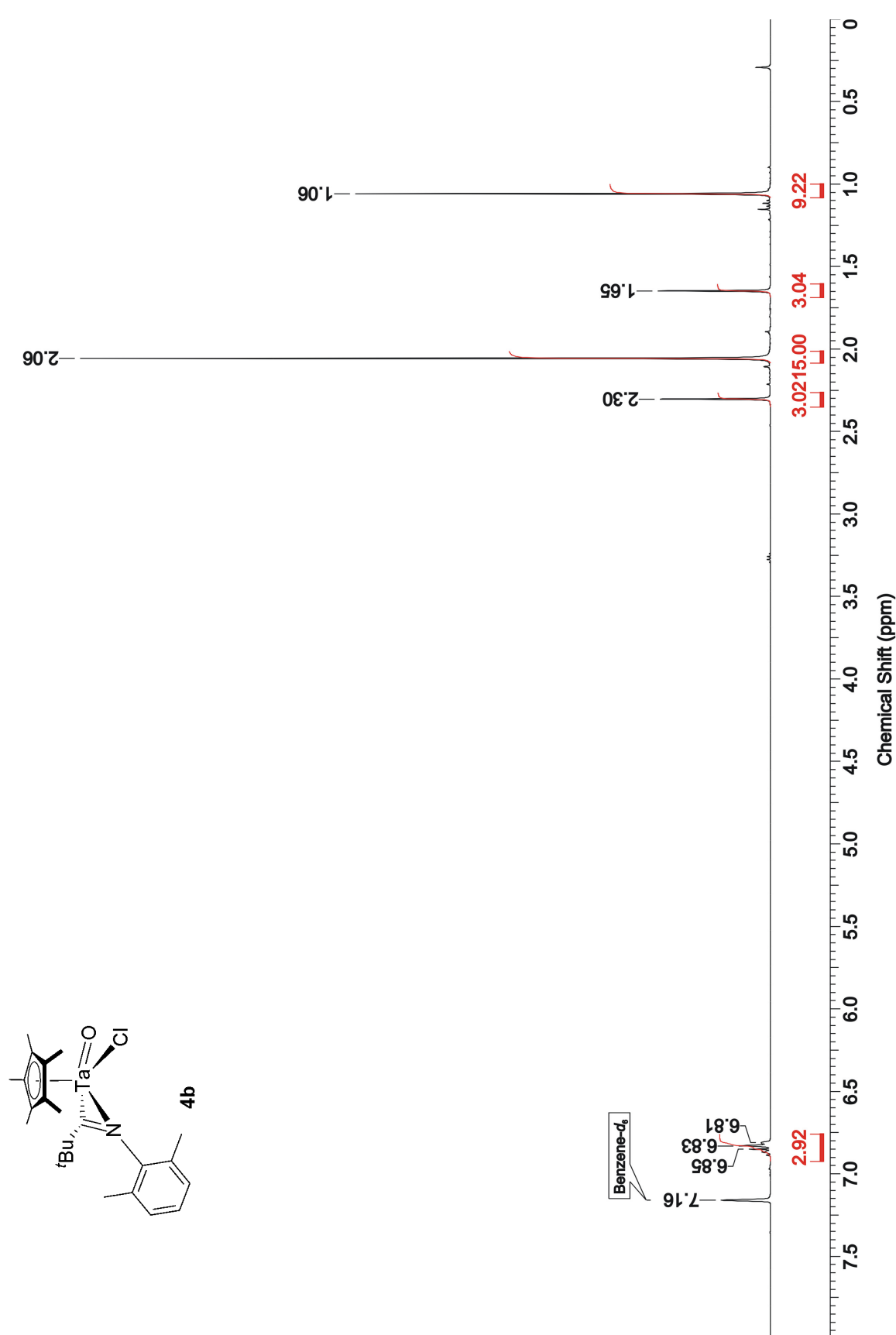


Figure S10. <sup>1</sup>H NMR spectrum (400MHz, RT) of **4b** in benzene-*d*<sub>6</sub>.

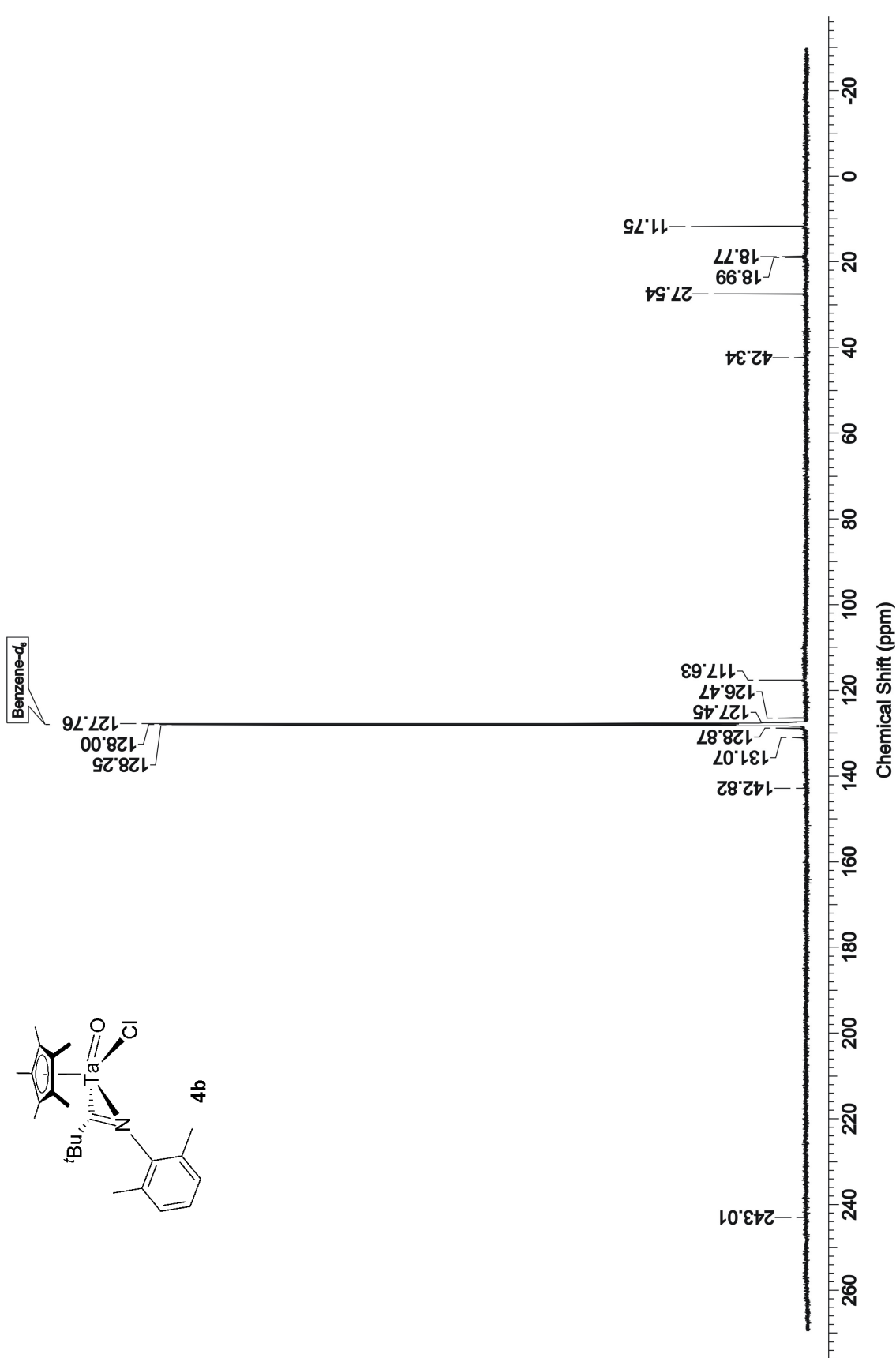


Figure S11.  $^{13}\text{C}$  NMR spectrum (100.6MHz, RT) of **4b** in benzene- $d_6$ .

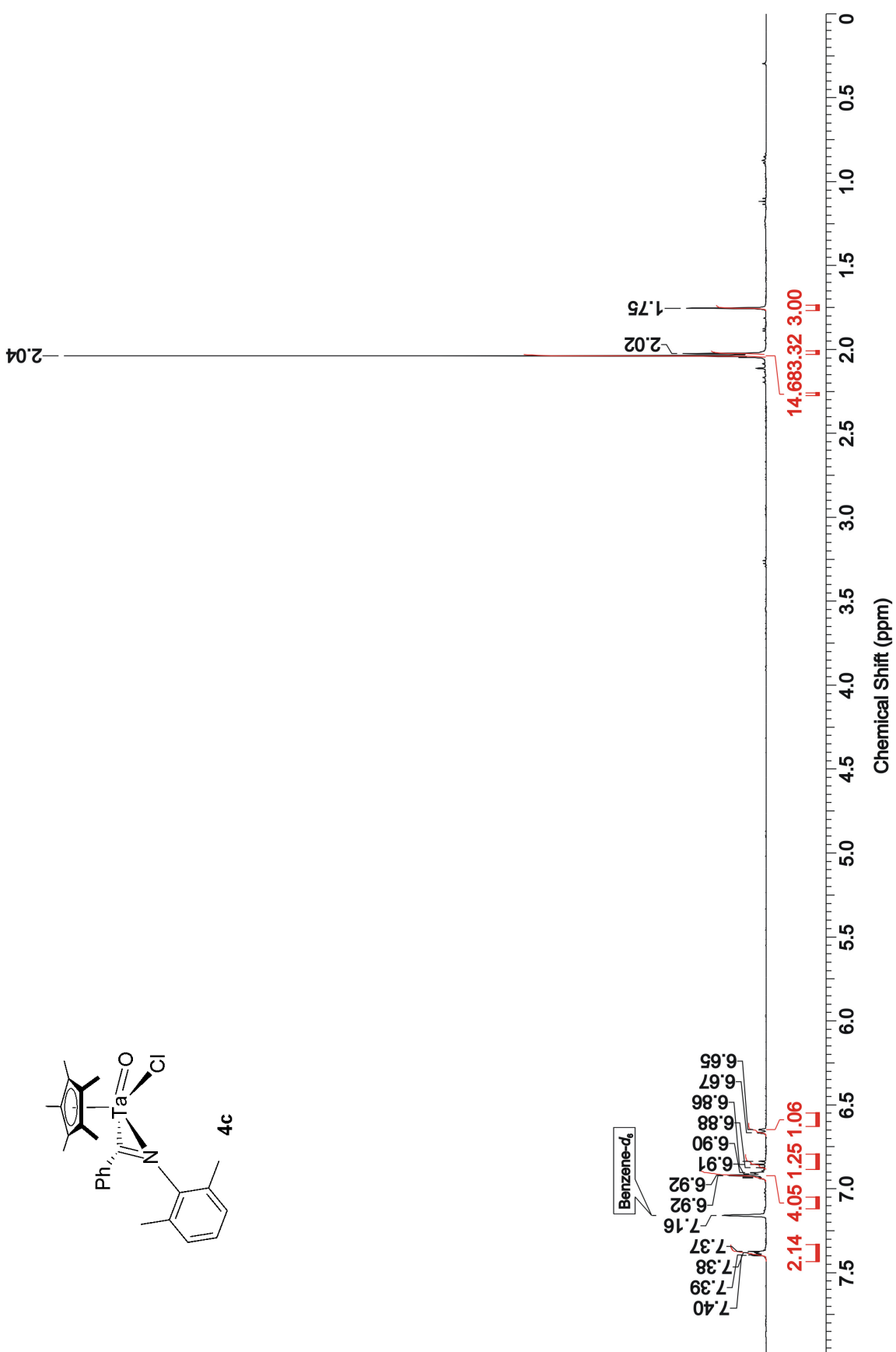


Figure S12. <sup>1</sup>H NMR spectrum (400MHz, RT) of **4c** in benzene-*d*<sub>6</sub>.

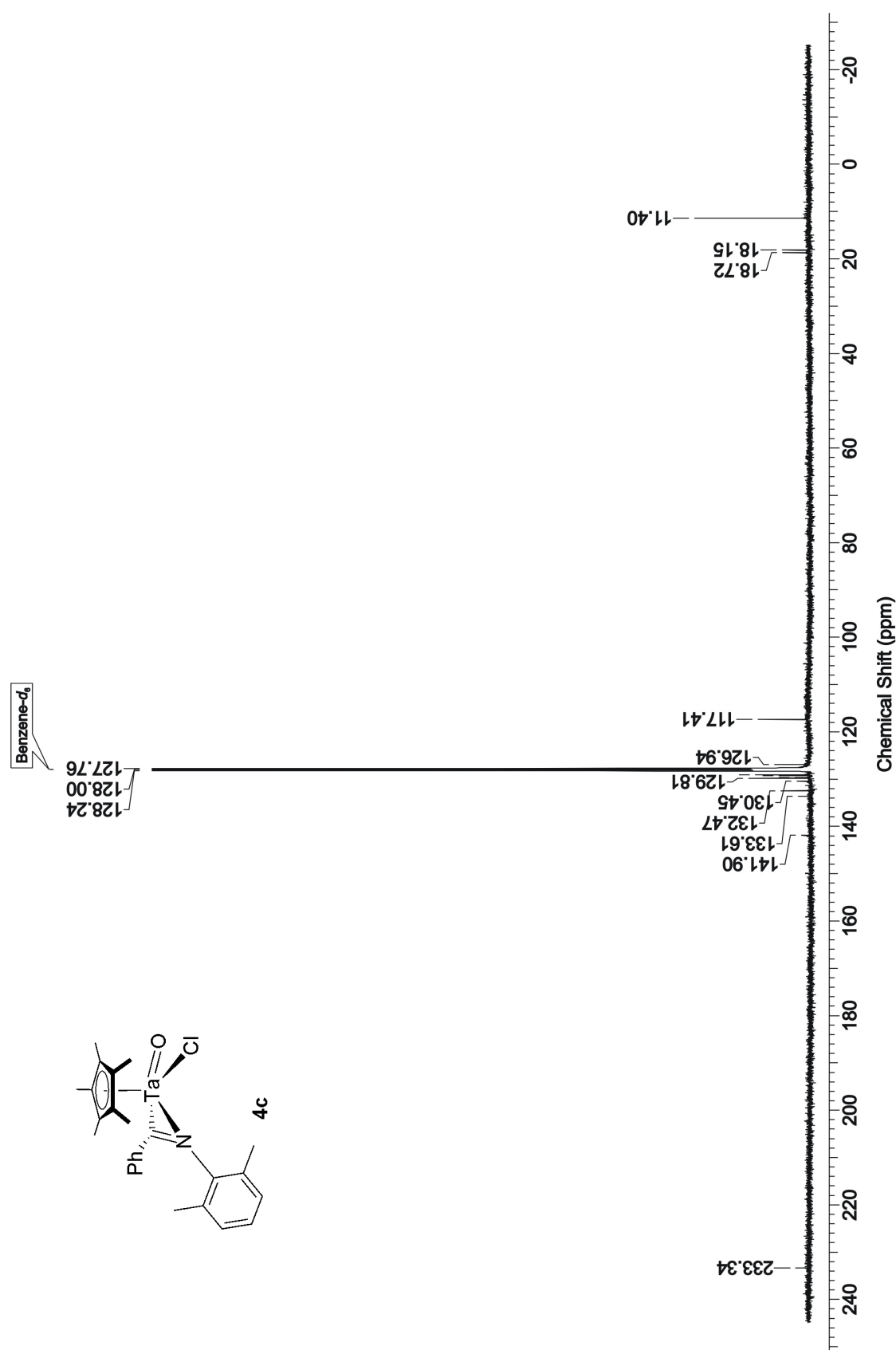


Figure S13.  $^{13}\text{C}$  NMR spectrum (100.6MHz, RT) of **4c** in benzene- $d_6$ .

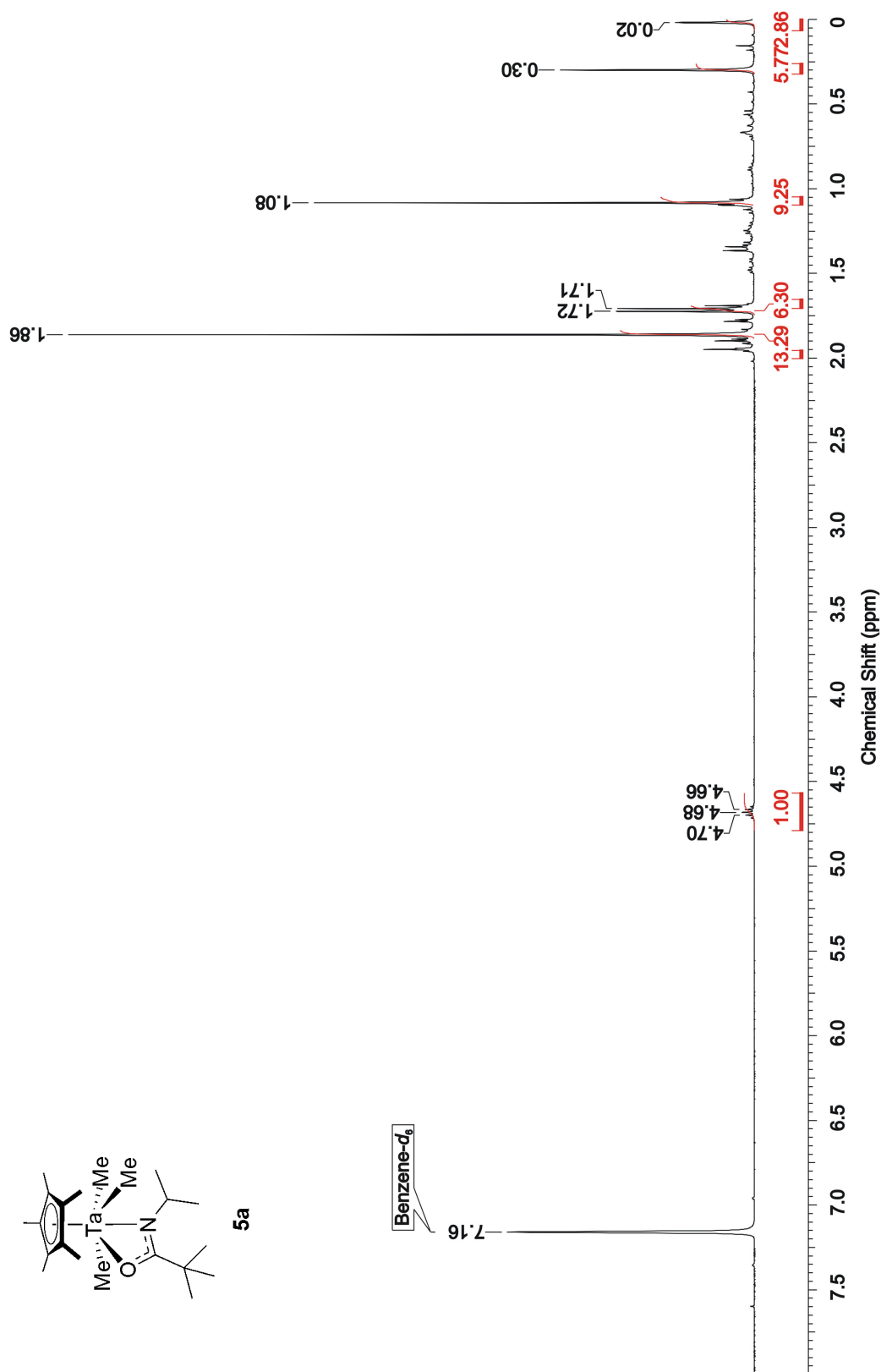
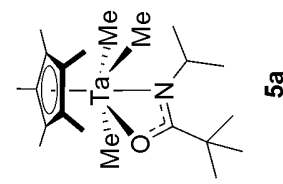


Figure S14. <sup>1</sup>H NMR spectrum (400MHz, RT) of **5a** in benzene-*d*<sub>6</sub>.

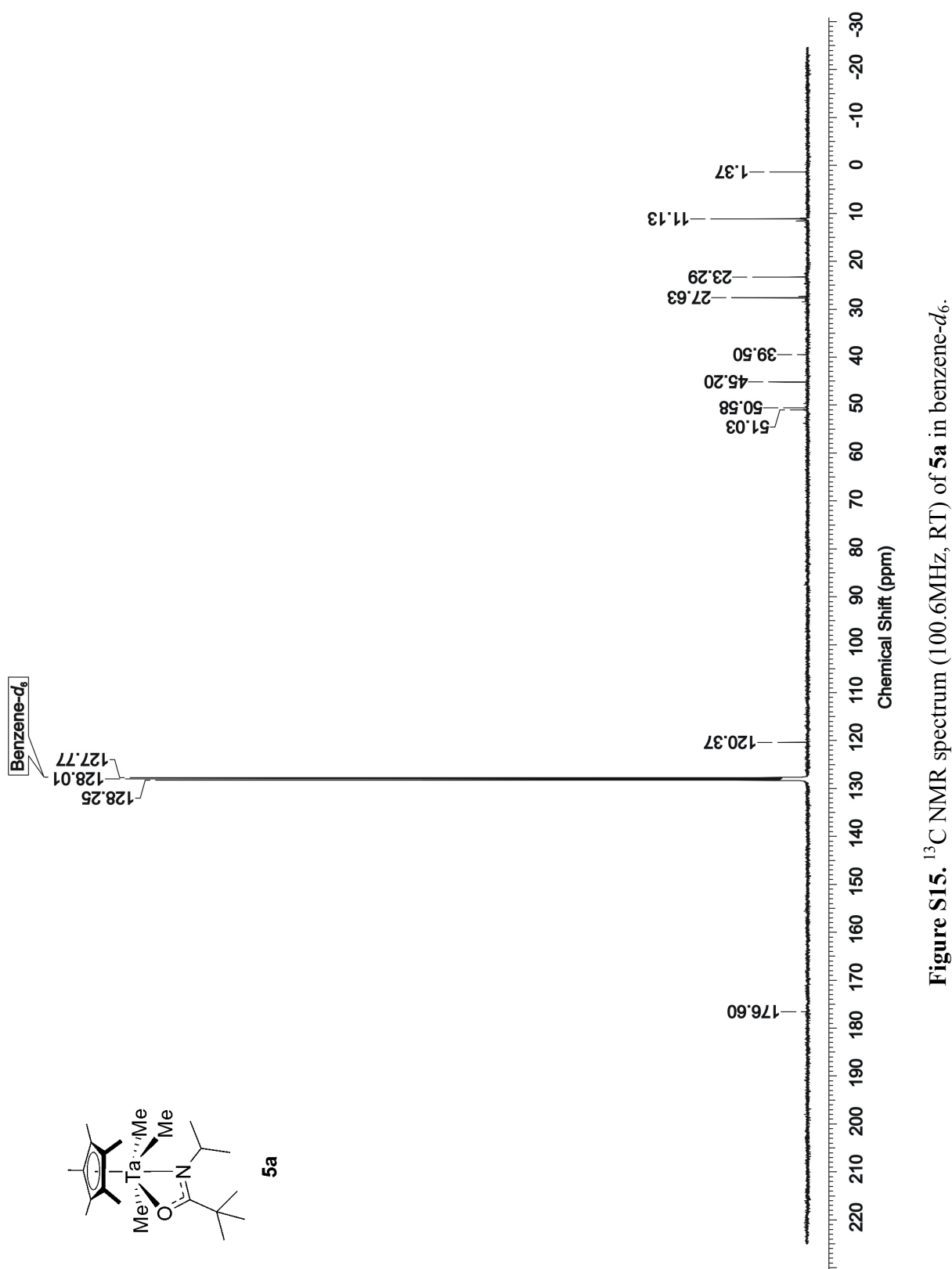


Figure S15.  $^{13}\text{C}$  NMR spectrum (100.6 MHz, RT) of **5a** in benzene- $d_6$ .

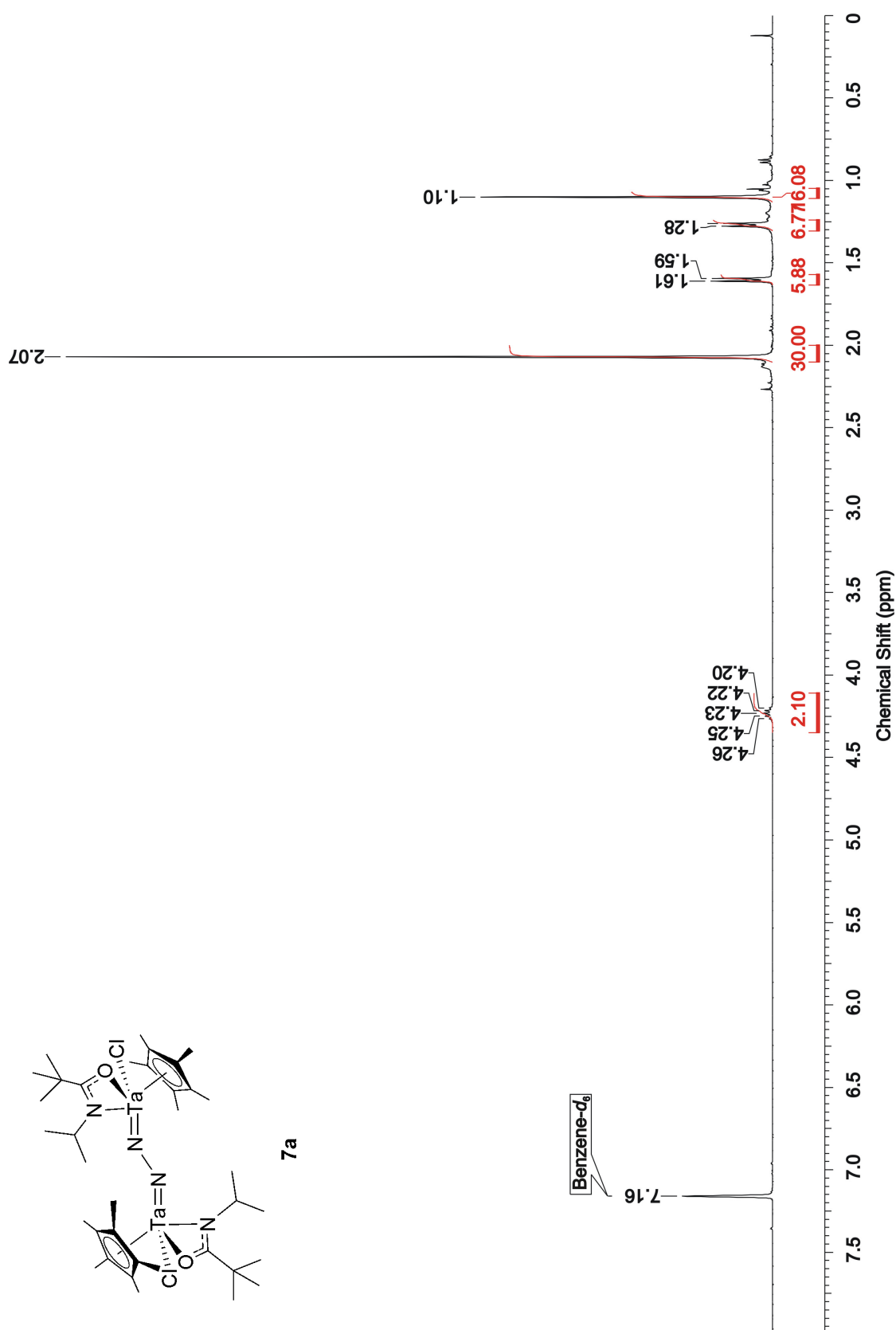


Figure S16.  $^1\text{H}$  NMR spectrum (400MHz, RT) of **7a** in benzene- $d_6$ .

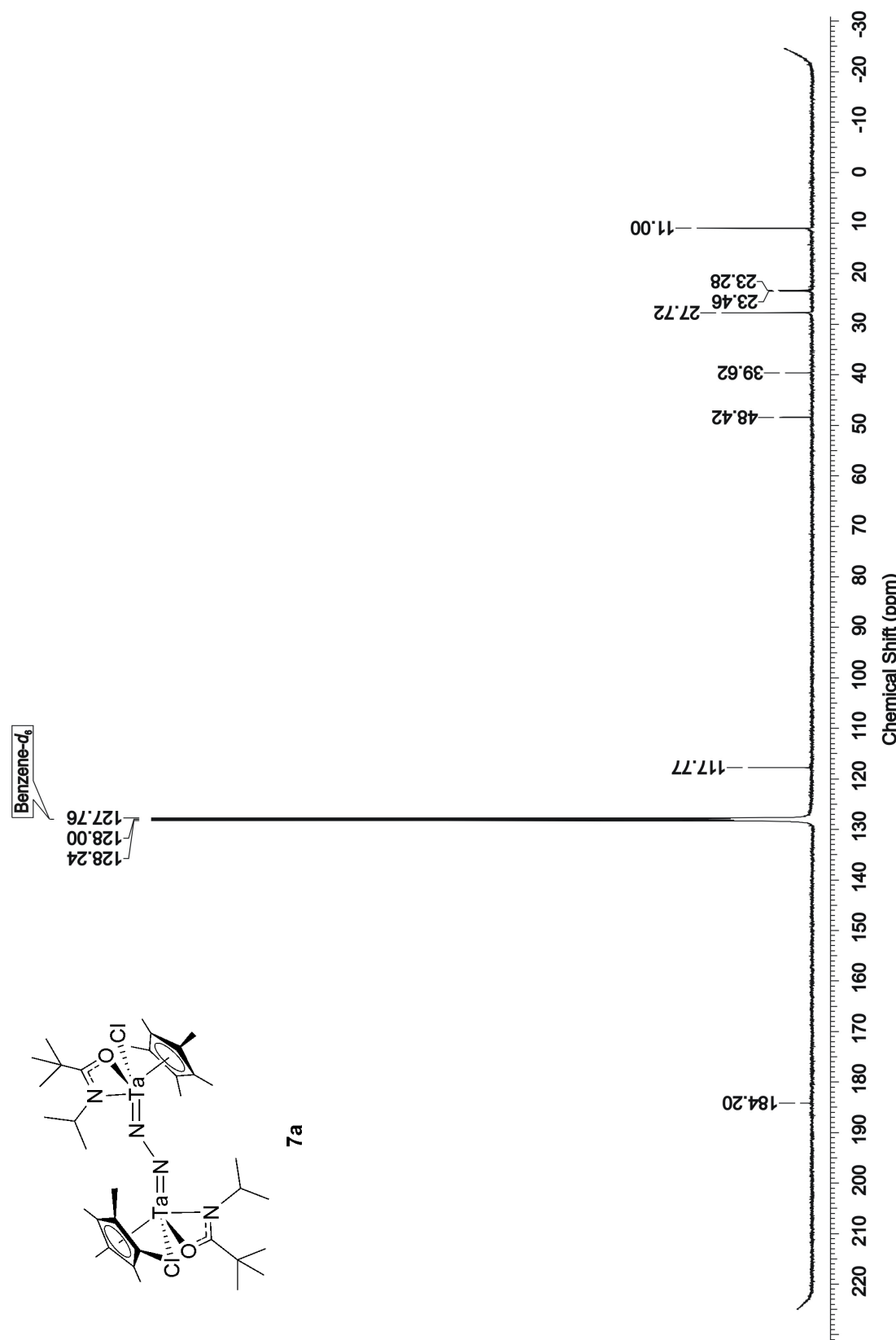


Figure S17.  $^{13}\text{C}$  NMR spectrum (100.6 MHz, RT) of **7a** in benzene- $d_6$ .

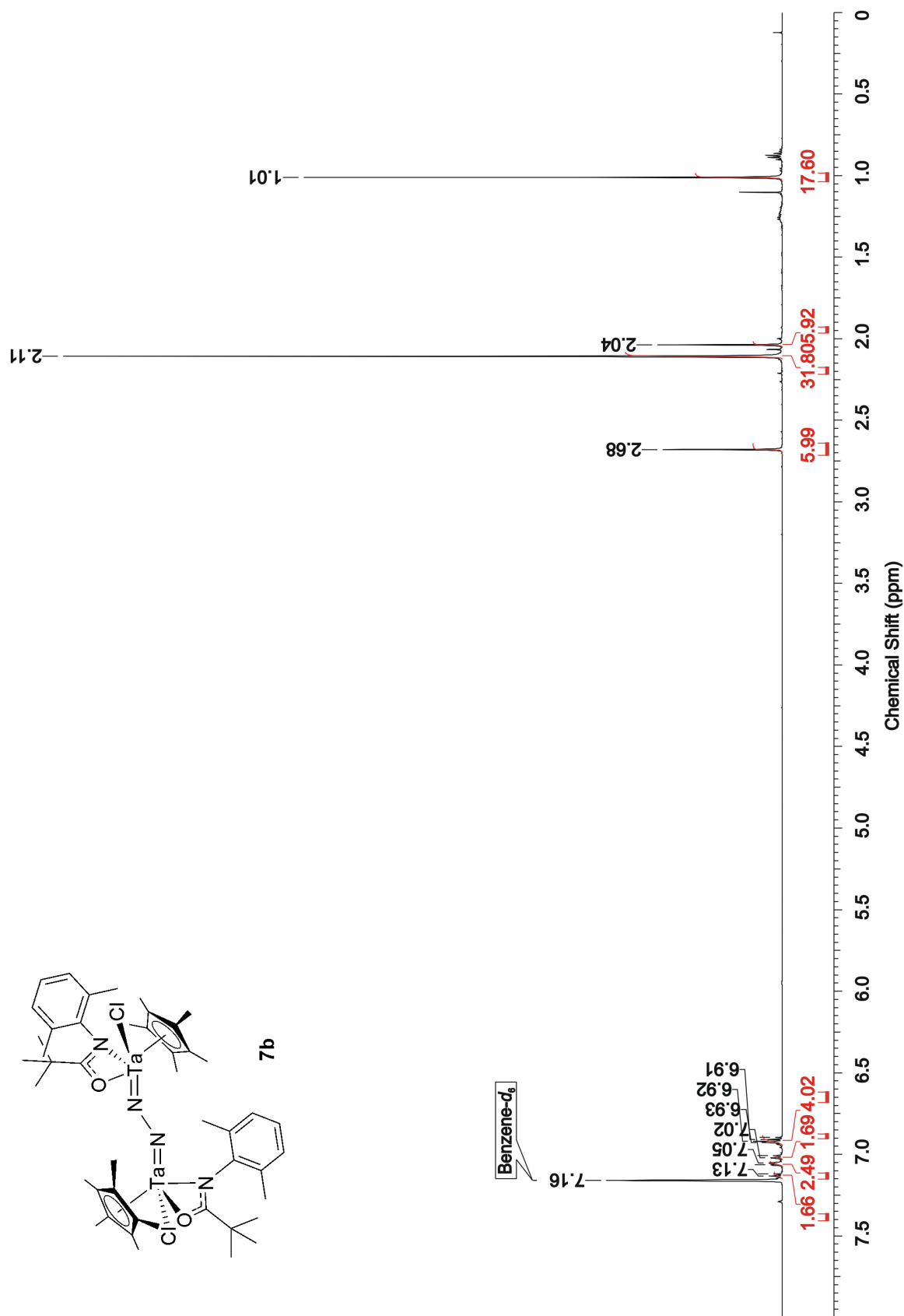
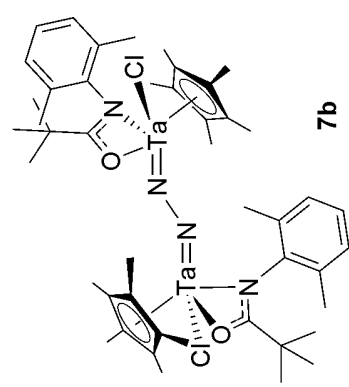


Figure S18.  $^1\text{H}$  NMR spectrum (600MHz, RT) of **7b** in benzene- $d_6$ .

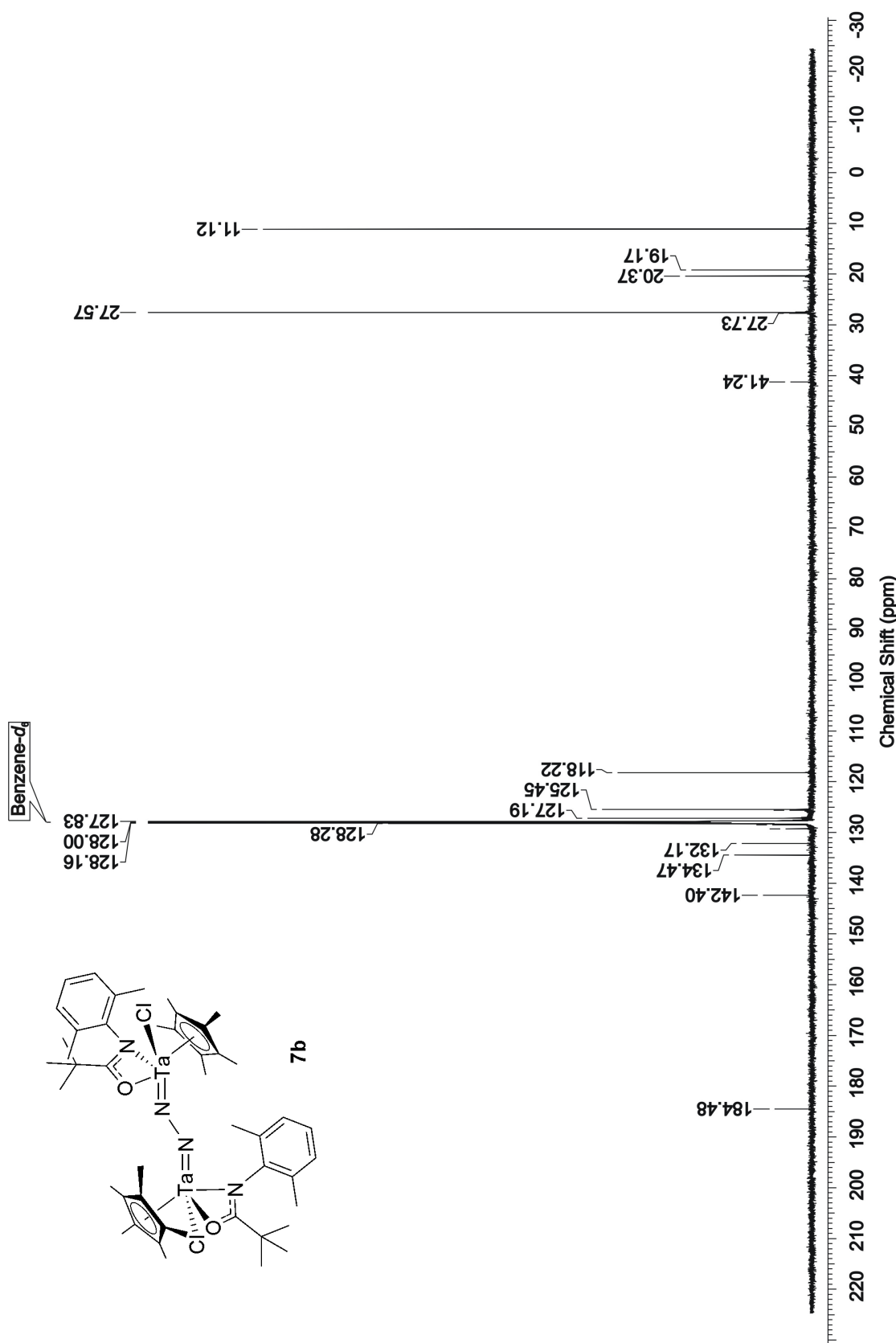


Figure S19.  $^{13}\text{C}$  NMR spectrum (150.9 MHz, RT) of **7b** in benzene- $d_6$ .